카복실기로 기능화된 다중벽 탄소 나노튜브의 첨가에 의한 PBT/PC 블렌드의 특성 개선

Yuanjiao Hu, Shixin Song, Xue Lv[†], and Shulin Sun[†]

Engineering Research Center of Synthetic Resin and Special Fiber, Ministry of Education,
Changchun University of Technology

(2017년 7월 6일 접수, 2017년 8월 20일 수정, 2017년 9월 21일 채택)

Enhanced Properties of PBT/PC Blends with the Addition of Carboxyl-functionalized Multiwalled Carbon Nanotube

Yuanjiao Hu, Shixin Song, Xue Lv[†], and Shulin Sun[†]

Engineering Research Center of Synthetic Resin and Special Fiber, Ministry of Education,
Changchun University of Technology, Changchun 130012, China
(Received July 6, 2017; Revised August 20, 2017; Accepted September 21, 2017)

Abstract: Carboxyl-functionalized multiwalled carbon nanotube (c-MWCNT) was used to enhance the properties of poly(butylene terephthalate)/polycarbonate (PBT/PC) blends by melt blending. The c-MWCNT inhibited transesterification reactions between PBT and PC. SEM result showed that most of the c-MWCNT dispersed in the PBT matrix and partial c-MWCNT lied between the interface of PBT and PC phases. c-MWCNT promoted the crystallization of PBT due to the decreased transesterification and the heterogeneous nucleating effect, which led to a 20 °C increase of the crystallization temperature. DMA test indicated that the miscibility between PBT and PC decreased with the c-MWCNT loading since the inhibited transesterification. When the c-MWCNT content was 4 wt%, the yield strength of 65.9 MPa and tensile modulus of 2116 MPa were achieved, which corresponded to 23.9 and 19.5% increase relative to the pure PBT/PC blend. The conductivity and dielectric properties of PBT/PC were largely enhanced by the c-MWCNT. The σ_{dc} values of PBT/PC improved greatly by several orders of magnitude from 10^{-18} to 10^{-7} when the c-MWCNT content was 2 wt%. The dielectric constant at 100 Hz for the nanocomposites increased from 2.8 to 146 when the c-MWCNT loading varied from 0.1 to 4 wt%, which improved more than 50 times.

Keywords: poly(butylene terephthalate), polycarbonate, carbon nanotube, nanocomposites.

Introduction

Polymer blending has become an important method to prepare novel materials with much better processability, chemical resistance, toughness and stiffness, electrical properties, and so forth.[1-7] For the polymer blends, aromatic polyester blends represent a major kind and have been investigated widely. poly(butylene terephthalate) (PBT) and polycarbonate (PC) blends belong to one important polyester pair, which combine the good balance of chemical and impact resistance, excellent flow characteristics and dimensional stability. PBT/PC blends have been used in automotive industry, outdoor power, appliance housings and so on.[8-14]

For the PBT/PC blends, most researches have been focused on the transesterification reactions, thermal properties, miscibility, phase morphology and impact modification.[15-19] Recently, nanocomposites based on PBT/PC blends attracted much attention. For example, Depolo and Baird investigated the effect of particle size of talc on dimensional stability and mechanical properties of PBT/PC blends. They found that using nanotalc instead of micro-size talc reduced the level of talc reinforcement from 6 to 1 wt% without sacrificing the coefficient of linear thermal expansion and shrinkage of injection-molded plaques. Furthermore, 14 and 120% improvement in the flexural strength and tensile toughness were achieved. Nanoclay has also been used to modify the PBT/PC blends. Compared to nano talc, nanoclay particles show much higher aspect ratio and lower density. It was found that by using only

[†]To whom correspondence should be addressed.
  pies112@126.com
  sunshulin1976@163.com ORCID 0000-0001-5341-1127

1 wt% nanocaly as opposed to nano-talc, the flexural strength and tensile toughness of the nanocomposites increased by 12 and 27%, respectively, and maintained a flexural modulus of 2.5 GPa.[20]

Among the nanofillers, carbon nanotube has been widely used to enhance the properties of polymers due to its unique and extraordinary thermal, mechanical and electrical properties.[21,22] The blends of carbon nanotube with PBT or PC have been prepared and investigated by some researchers.[23-25] As for the PBT nanocomposites, carbon nanotube improved the crystallization rate and degree. At the same time, the PBT blends showed much higher stiffness, thermal stability and conductivity. Similar with the PBT nanocomposites, carbon nanotube modified PC blends also showed improved modulus and strength, enhanced chemical resistance and thermal properties.

Not only the carbon nanotube properties but also the preparation method can affect the electrical properties of PC. The PC/c-MWCNT nanocomposites with different percolation threshold (P_c) have been reported by some researchers. Though PBT/PC blends have been studied for many years and used widely in many engineering applications, few reports on the carbon nanotube modified PBT/PC blends could been found from the literatures. S. Maiti *et al.* used PBT to decrease the percolation threshold of PC/multiwalled carbon nanotubes. It was found that only 0.35 wt% multiwalled carbon nanotubes were enough to improve the conductivity of the nanocomposites.[26] Yu *et al.* used carbon nanotube to improve the conductivity of PBT/PC blends. They found that the carbon nanotube distributed in the PBT phase and the conductive materials were obtained with 1 wt% carbon nanotube addition.[27] Elastomer particles and carbon nanotubes were utilized by Wang *et al.* to improve the toughness of PBT/PC blends. They pointed out that the elastomer particles (SEBS-*g*-MA) enhanced the impact strength of PBT/PC blend. Furthermore, the introduction of carbon nanotube improved the toughening efficiency of SEBS-*g*-MA for PBT/PC blends.[28] Different with these researches, carboxyl-functionalized multiwalled carbon nanotube (c-MWCNT) was used to improve the properties of PBT/PC blends. The carboxyl groups on the carbon nanotube increase the polarity which should be beneficial to enhance the miscibility between carbon nanotube and the polyester matrix. Furthermore, the inhibition of transesterification in PBT/PC blends due to the c-MWCNT was firstly reported and the dielectric properties were studied in detail, which have not been reported in the above papers. In the present paper, the effect of carboxyl-functionalized multiwalled carbon nanotube

on the mechanical properties, morphology, crystallization, conductive and dielectric properties of PBT/PC blends was investigated in detail.

Experimental

Materials. The PBT was purchased from the Engineering Plastics Plant of Yihua Group Corp., China. The PC used was a commercial product of Bayer Plastics designated as Makrolon 2805. c-MWCNT was purchased from Chengdu Institute of Organic Chemistry, Chinese Academy of Science (Chengdu, P.R. China). The outer and inner diameters of c-MWCNT are 10~20 and 5~10 nm, respectively. The length of a single c-MWCNT is about 10~30 μm and the -COOH content is 2 wt%.

Preparation of the Nanocomposites. The PBT/PC/c-MWCNT nanocomposites were prepared by melt blending method. The PC, PBT and c-MWCNT were dried in a vacuum oven at 80 °C for 24 h before processing to remove the moisture. The blending was carried out in a Thermo Haake internal mixer. The temperature was set at 240 °C with a rotation speed of 55 rpm and the mixing time was 5 min. The composition of PBT/PC/c-MWCNT nanocomposites was listed in Table 1. After blending, the samples with different compositions were obtained by hot press molding for 3 min at 240 °C and cold press molding for 3min at room temperature.

Morphological Properties. SEM micrographs were obtained with a JSM6510 scanning electron microscope (JEOL, Japan) with an operation voltage of 10 kV. Before testing, the samples were frozen in liquid nitrogen for 3 h and then fractured. The fracture surface of the samples was coated with a gold layer for SEM observation.

Differential Scanning Calorimetry (DSC). Perkin-Elmer DSC-7 was used to study the melting and crystallization behavior of PBT/PC/c-MWCNT nanocomposites. The sam-

Table 1. The Composition of PBT/PC/c-MWCNT Nanocomposites

(unit: wt%)

Designation	PBT content	PC content	c-MWCNT content
PBT/PC	50	50	0
Blend-CNT0.1	49.95	49.95	0.1
Blend-CNT0.5	49.75	49.75	0.5
Blend-CNT1	49.5	49.5	1
Blend-CNT2	49	49	2
Blend-CNT3	48.5	48.5	3
Blend-CNT4	48	48	4

ples were heated from 30 to 240 °C at 10 °C/min and held for 3 min at 240 °C, then cooled from 240 to 30 °C at 10 °C/min. The tests were under a nitrogen atmosphere.

Dynamic Mechanical Analysis (DMA). The blends were compression molded at a melting temperature of 240 °C to obtain plates that were suitable for the DMA test. These plates were sized $30 \times 4 \times 1$ mm³. The sample was tested on a Perkin Elmer dynamic mechanical analyzer. The sample was heated from 30 to 260 °C at a heating rate of 3 °C/min and a frequency of 1 Hz.

Mechanical Properties. The uniaxial tensile tests were carried out at 23 ± 2 °C on an Instron 3365 tensile tester at a crosshead speed of 50 mm/min according to the ASTM D638 standard. The notched Izod impact strength of the blends was measured by an XJU-22 Izod impact tester at 23 ± 2 °C according to the ASTM D256 standard. For both mechanical tests, at least five samples were dried overnight prior to testing until the measurement was performed.

Electrical Conductivity and Dielectric Properties. Direct-current electrical conductivity (σ_{dc}) measurements were done on molded specimen (diameter: 80 mm, thickness: 1 mm). The electrical conductivity of the conducting nanocomposites was measured with the digital type high resistance calibrator.

Alternating-current electrical conductivity (σ_{ac}) and dielectric properties of the nanocomposites were obtained with a computer-controlled precision impedance analyzer (Agilent E4980A, 16451B). The frequency ranged from 20 to 10^6 Hz. The dielectric constant (ε') and dielectric loss tangent (tanδ) were obtained as a function of frequency. The σ_{ac} was calculated from the dielectric data with the following equation[26]:

$$\sigma_{ac} = \omega \varepsilon_0 \varepsilon' \tan\delta$$

where ω is the angular frequency which is equal to $2\pi f$ (where f is the frequency), ε_0 is the vacuum constant, ε' is the dielectric constant and tanδ is the dielectric loss tangent.

Results and Discussion

Transesterification Analysis. The transesterification reactions between PBT and PC have been investigated widely. The previous researches in our group have proved that transesterification reactions took place in the present processing condition for the PBT/PC blends.[11-14] In this part, the influence of c-MWCNT on the transesterification reactions was analyzed by FTIR test. Figure 1(a) shows the FTIR results of pure PBT and PC. The C=O stretching bands of the carbonyl group in neat PC and PBT were 1775 and 1710 cm⁻¹, respectively. Figure 1(b) shows the FTIR results of extracted insoluble PBT/PC samples with different c-MWCNT content. The absorption peak at 1775 cm⁻¹ for the PC phase can be found in the FTIR spectra for the insoluble portion of the extracted PBT/PC blends. It is believed that this peak is associated with the C=O stretching of the PC segments in the PBT-*b*-PC copolymer in the insoluble portion. FTIR results testify the occurrence of transesterification reactions between PBT and PC. On the other hand, the addition of c-MWCNT decreases the C=O peak intensity of PC phase compared with the extracted PBT/PC FTIR result. FTIR result shows that c-MWCNT can inhibit the transesterification, but the transesterification can't be fully suppressed with the addition of c-MWCNT.

Morphology. The dispersed morphology of nanofiller in the polymers is very important for the properties of the nanocomposites. In most blends, the uniform dispersion of the nanofiller is beneficial to the properties improvement. Figure 2
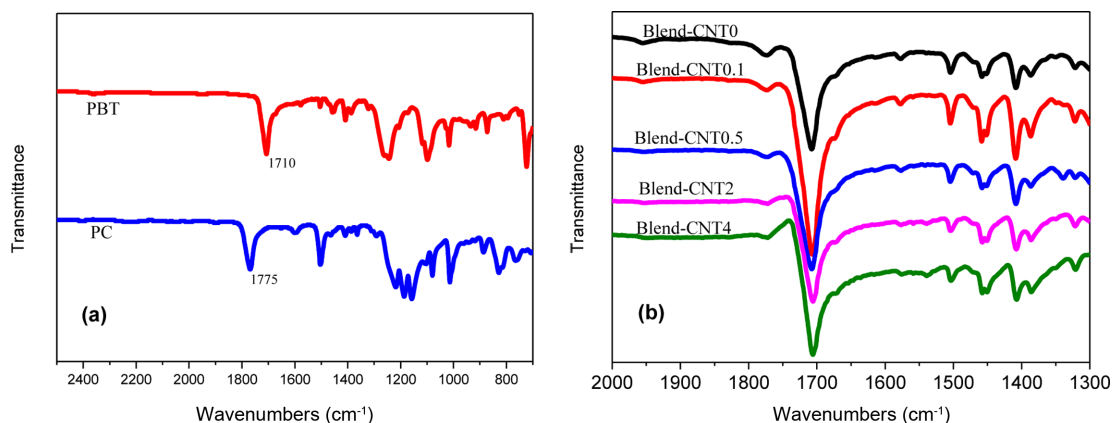

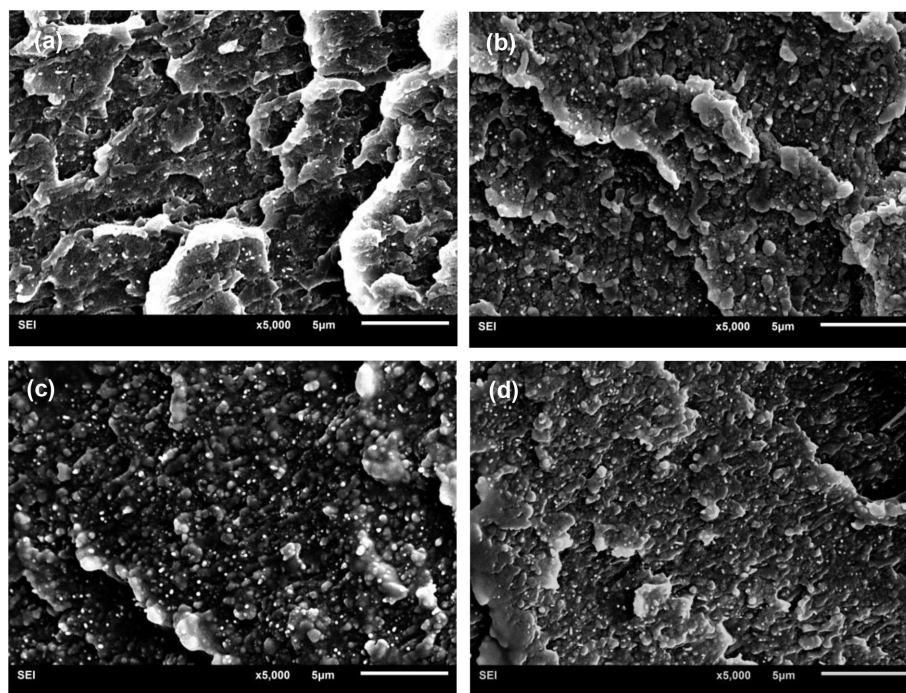**Figure 1.** FTIR of PBT, PC (a); the extracted PBT/PC blends (b).

Figure 2. Dispersed morphology of c-MWCNT in the PBT/PC blends. (a) Blend-CNT1; (b) Blend-CNT2; (c) Blend-CNT3; (d) Blend-CNT4.

shows that partial c-MWCNTs disperse in the PBT/PC matrix uniformly and local agglomeration also can be found in some domains.

Figure 3 shows the etched SEM phase morphology and TEM of PBT/PC and Blend-CNT2 blends. The PC phase was etched by methylene dichloride. In Figure 3(a), the PBT forms the continuous phase and the PC disperses in the PBT matrix. Phase separation takes place obviously for PBT and PC, which indicates that PBT and PC are immiscible in this research. When c-MWCNTs are added into the PBT/PC blends, phase separation also occurs according to the etched morphology of PC phase (Figure 3(b)). On the other hand, most of the c-MWCNTs disperse in the PBT phase from the Figures 2 and 3. Furthermore, partial c-MWCNTs lie between the interface of PBT and PC phases according to Figures 2 and 3(c) (see the red circles in Figure 3(c)). The SEM and TEM morphology proves that c-MWCNT shows much higher affinity with PBT phase and similar result has been reported in other research.[27]

DSC Analysis. Figure 4 shows the crystallization behavior of PBT and the PBT/PC/c-MWCNT nanocomposites. It can be found that the crystallization temperature (T_c) of pure PBT is about 199.8 °C. The T_c of PBT in the PBT/PC blend decreases to 191.5 °C. The decease of T_c for PBT phase in the PBT/PC blends is due to the transesterification reaction between PBT to

PC and similar results have been reported in many researches.[29-31] In the PBT/PC/c-MWCNT blends, the T_c of PBT phase increases obviously compared to the value in the PBT/PC blend and even 0.1% c-MWCNT induces a 14 °C improvement. When the c-MWCNT content is 4% (T_c=211.8 °C), the T_c is enhanced more than 20 °C. Two reasons can be used to explain the crystallization change of PBT in the nanocomposites. Firstly, the addition of c-MWCNT inhibits the transesterification reaction between PBT and PC which decreases the constraint of PC on the PBT crystallization process. Secondly, the c-MWCNT plays the role of heterogeneous nucleating agent which promotes the crystallization of PBT. The increase of T_c indicates that the c-MWCNT enhances the crystallization rate of PBT in the PBT/PC/c-MWCNT nanocomposites.

Figure 5 shows the melting behavior of PBT and the PBT/PC/c-MWCNT nanocomposites. It can be found that pure PBT shows one main melting peak (T_m=230.8 °C) and a small melting peak (T_m=220.3 °C). The small melting peak attributes to the partial melting of the less perfect crystals and the main melting peak attributes to the melting of the original and recrystallized crystals.[31-33] In the PBT/PC/c-MWCNT blends, the small melting peak disappears and only the main melting peak exists. Compared to the main melting temperature (T_m) of
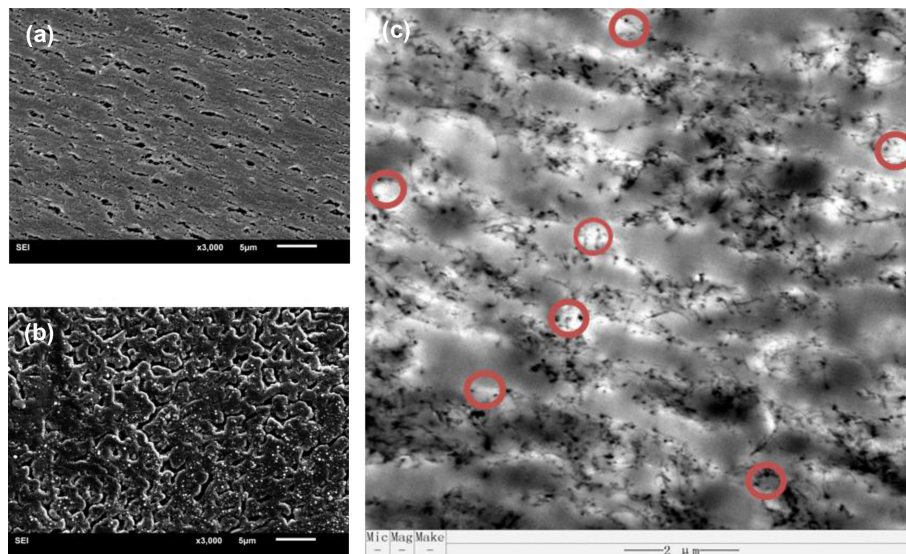
Figure 3. Influence of c-MWCNT on the phase morphology of PBT and PC: (a) PBT/PC (SEM); (b) Blend-CNT2 (SEM); (c) Blend-CNT2 (TEM).
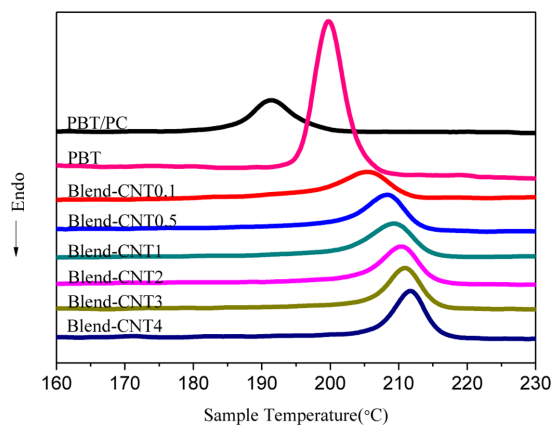

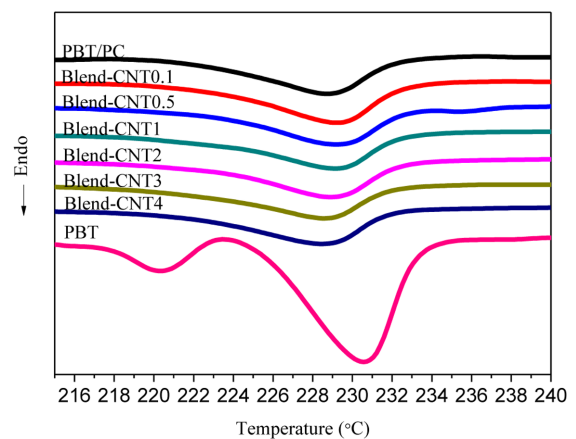**Figure 4.** Crystallization behavior of PBT and the PBT/PC/c-MWCNT nanocomposites.

Figure 5. Melting behavior of PBT and the PBT/PC/c-MWCNT nanocomposites.

pure PBT, the T_m of PBT phase moves to lower temperature in the nanocomposites. The change of c-MWCNT content in the PBT/PC blends has no obvious influence on the melting behavior.

DMA Analysis. The pure PBT amorphous phase and PC show the T_g peaks at 53 and 152 °C, respectively (Figure 6(a)). As for the PBT/PC blends in Figure 6(b), the T_g of the PBT phase moves to higher temperature (65 °C) and the T_g of the PC phase shifts to lower temperature (119 °C) compared with pure PBT and PC which indicates the partial miscibility between PBT and PC due to the transesterification reaction. However, the addition of c-MWCNT changes the T_g of PBT and PC phases obviously in the nanocomposites. With the

increase of c-MWCNT content in the blends, the T_g of the PBT phase shifts to lower temperature and the T_g of the PC phase shifts to higher temperature. Two reasons can be used to explain the T_g change of PBT and PC in the nanocomposites. Firstly, the addition of c-MWCNT inhibits the transesterification reaction between PBT and PC which decreases the miscibility between PBT and PC and induces the T_g move to the original T_g of the pure polyesters. Secondly, the high aspect ratio of c-MWCNT in the matrix leads to strong interfacial interaction between c-MWCNT and the polyesters. The nanometric dimension of the c-MWCNT in the blends contributes to the process of tether chain entanglement which decreases polymer chain relaxation and induces higher T_g of the polymers.
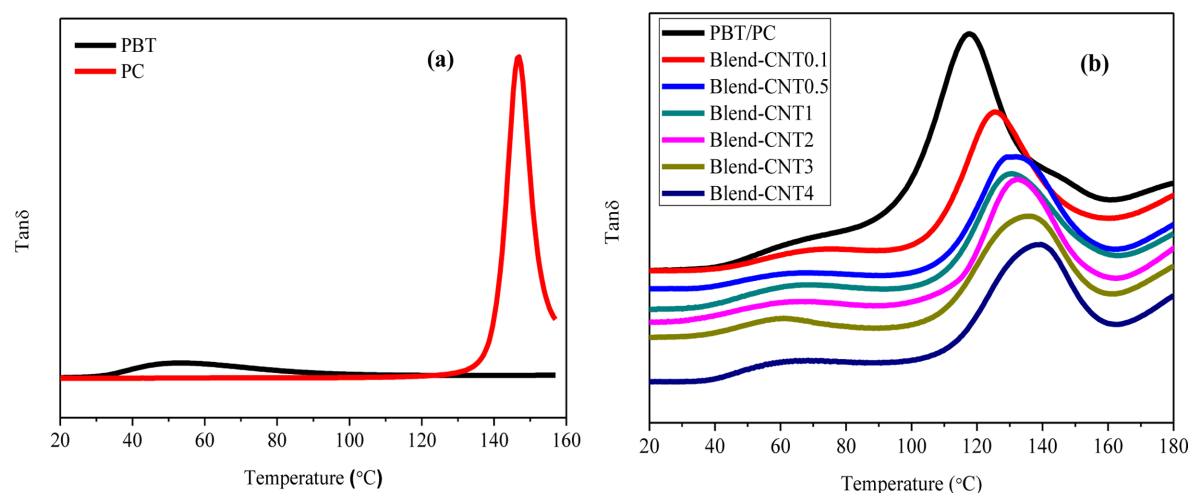
Figure 6. Tan δ and temperature relationship curves of PBT/PC/c-MWCNT.
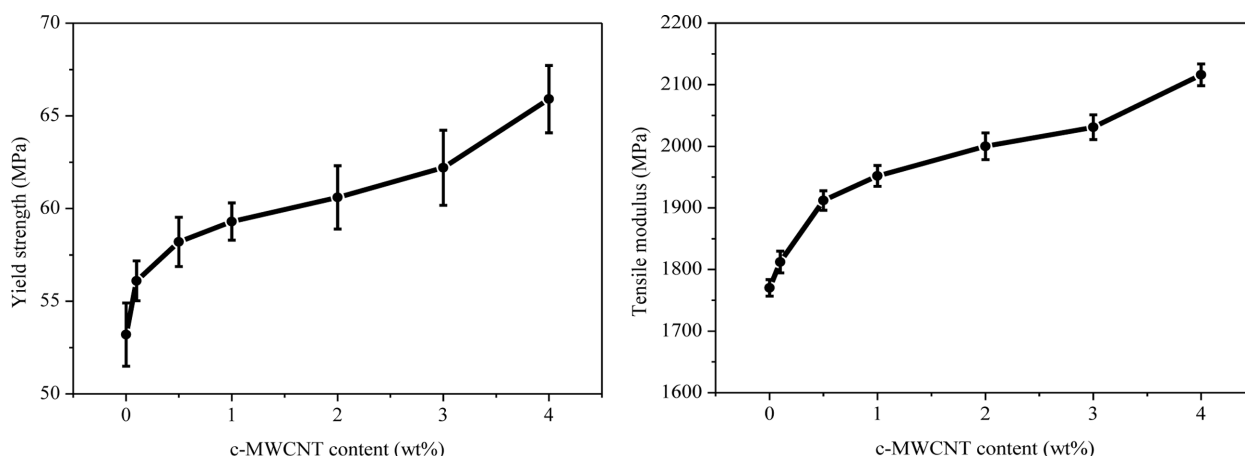

Figure 7. Influence of c-MWCNT on the mechanical properties of PBT/PC blends.

Mechanical Properties. Table 2 shows the mechanical properties of PBT/PC blends with varied PBT and PC compositions. It can be found that PBT displays lower yield strength and tensile modulus than PC. The yield strength and tensile modulus increase with the improvement of PC content in the PBT/PC blends. Since the PBT/PC blend with the 50/50 composition shows good mechanical properties and which combines the essential properties of pure PBT and PC phases, the PBT/PC with 50/50 composition is selected as the basic ratio for the PBT/PC/c-MWCNT blends.

The influence of c-MWCNT on the mechanical properties of

PBT/PC blends was investigated. The yield strength and tensile modulus of PBT/PC blend are 53.2 and 1770 MPa, respectively. In Figure 7, it can be found that the yield strength and tensile modulus increase obviously with the c-MWCNT content. When the c-MWCNT content is 4 wt%, the yield strength of 65.9 MPa and tensile modulus of 2116 MPa are achieved, which correspond to 23.9 and 19.5% increase relative to the pure PBT/PC blend. The improvement for the mechanical properties of PBT/PC blends is due to the reinforcing effect of c-MWCNT and the improved crystallization properties of PBT. The addition of c-MWCNT is beneficial to the mechan-

Table 2. Mechanical Properties of PBT/PC Blends with Varied PBT and PC Compositions (unit: MPa)

PBT/PC (wt/wt)	100/0	90/10	70/30	50/50	30/70	10/90	0/100
Yield strength	51.3±1.1	51.9±0.7	52.6±1.0	53.2±1.2	54.3±0.8	55.8±1.3	57.2±0.9
Tensile modulus	1530±25	1586±17	1675±31	1770±13	1832±24	1893±32	1920±29
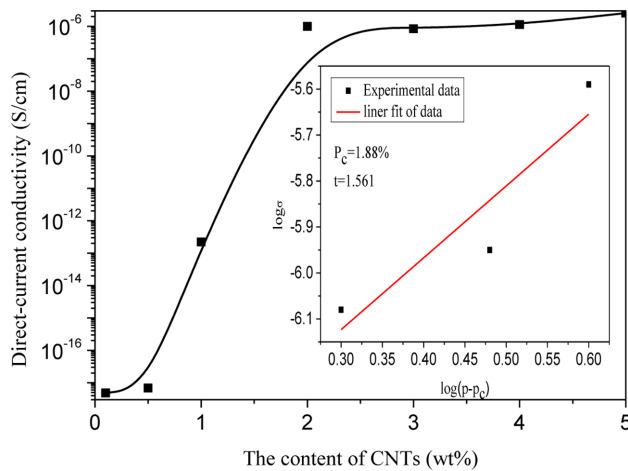
Figure 8. σ_{dc} *versus* c-MWCNT concentration for PBT/PC/c-MWCNT nanocomposites.

Figure 9. Dependence of the frequency on the AC conductivity for the PBT/PC/c-MWCNT nanocomposites.

Figure 10. Dependence of the dielectric constant on frequency for PBT/PC/c-MWCNTs nanocomposites.

ical properties of PBT/PC blends.

Conductivity. In Figure 8, the σ_{dc} value of PBT/PC/c-MWCNT nanocomposite is 4.83×10^{-18} s/cm with 0.1 wt% c-MWCNT addition, which is similar with the conductivity of the insulating PBT/PC matrix. The conductivity of the nanocomposite increases with the c-MWCNT content. The σ_{dc} values of PBT/PC/c-MWCNT nanocomposites improves greatly by several orders of magnitude from 10^{-18} to 10^{-7} when the nanocomposite is prepared with 2 wt% loading of c-MWCNT. This obvious jump in the conductivity definitely indicates the formation of a continuous conductive interconnected network path of c-MWCNT in the nanocomposites, which has been well known as a percolation network. According to the statistical percolation theory, the value of percolation threshold (p_c) is obtained by fitting the variation of electrical conductivity (σ) with c-MWCNT concentration (p) using the scaling law: $\sigma = \sigma_0 (p-p_c)^t$

Figure 8 shows the $\log\sigma$ *versus* $\log(p-p_c)$ plot and the values of the critical exponent t and critical c-MWCNT concentration p_c can be calculated. In the present research, the p_c is 1.88 wt% and t is 1.561. Figure 9 shows the variation of the AC electrical conductivity with the frequency in the frequency region of $2 \times 10^1 - 10^6$ Hz for the PBT/PC/c-MWCNT nanocomposites measured at room temperature. When the content of c-MWCNT is below 2 wt%, the conductivity of the nanocomposites shows a linear relationship with the frequency, which is the typical property for insulators. However, the conductivity displays a sudden jump from 10^{-12} to 10^{-7} at 20 Hz when the c-MWCNT content increases to 2 wt%. Furthermore, at low frequency, the conductivity of the nanocomposite is
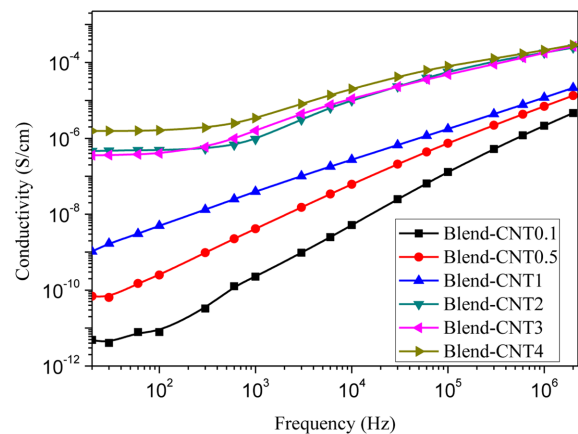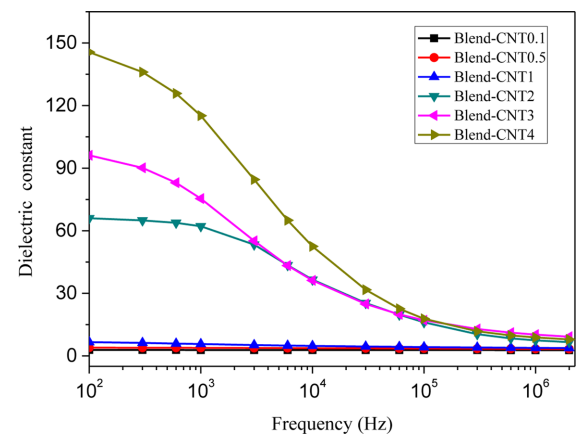
independent on the frequency and begins to increase at higher frequency. With the increase of the c-MWCNT content, the transition region moves to higher frequency. Similar phenomena have been found in other percolative composites.[34-36]

Dielectric Properties. Figure 10 shows the plots of the dielectric constant as the function of frequency for PBT/PC/c-MWCNT nanocomposites with various weight ratios of c-MWCNT. The dielectric constant of the nanocomposites with small c-MWCNT content is low and which is frequency independent. When the content of c-MWCNT is more than 2 wt%, the dielectric constant rises significantly. The dielectric constant at 100 Hz for the nanocomposites increases from 2.8 to 146 when the c-MWCNT loading varies from 0.1 to 4 wt%, which improves more than 50 times. On the other hand, the dielectric constant decreases with the increasing frequency at high-frequency zone. According to the minicapacitor model,
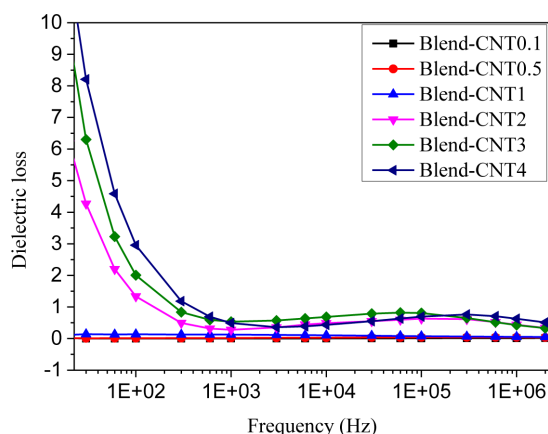
Figure 11. Dependence of the dielectric loss on frequency of PBT/PC-cMWCNTs nanocomposites.

when the c-MWCNT content is lower than P_c, the c-MWCNTs are separated by the polymer layers and form some mini-capacitors, which improve the dielectric constant of the PBT/PC/c-MWCNT nanocomposites. Furthermore, c-MWCNTs connect together and form the conductive network when the content of c-MWCNTs is beyond P_c. So the dielectric constant of the PBT/PC/c-MWCNT nanocomposites increases significantly when c-MWCNT content is higher than P_c.

Figure 11 shows the plots of dielectric loss *vs.* frequency for the PBT/PC/c-MWCNT nanocomposites with the different contents of c-MWCNT. Similar with other conductive filler/polymer nanocomposites, when the loading of conductive fillers are larger than P_c,[37,38] the dielectric loss of the PBT/PC/c-MWCNTs nanocomposites mainly consists of the loss of electric conduction and the loss of interfacial polarization. As the loss of electric conduction makes more contribution to dielectric loss than that of interfacial polarization at relatively low frequency, the dielectric loss of nanocomposites decreases with increase in the frequency.

Conclusions

In this work, poly(butylene terephthalate)/polycarbonate (PBT/PC) nanocomposites with carboxyl-functionalized multiwalled carbon nanotube (c-MWCNT) as modifier were prepared by melt blending method. FTIR results testified the inhibited transesterification between PBT and PC due to the c-MWCNT loading. The carboxyl groups on the carbon nanotube increased the polarity which was beneficial to enhance the miscibility between carbon nanotube and the polyester matrix. c-MWCNT enhanced the crystallization temperature of PBT

due to the decreased transesterification and the heterogeneous nucleating effect but had no obvious influence on the melting behavior. The increase of c-MWCNT content led the T_g of the PBT phase shift to lower temperature and the T_g of the PC phase shift to higher temperature. The reasons lied in the inhibited transesterification and strong interfacial interaction between c-MWCNT and the polyesters. The addition of c-MWCNT was beneficial to the mechanical properties of PBT/PC blends. The yield strength and tensile modulus of the nanocomposites showed 23.9 and 19.5% increase relative to the pure PBT/PC blend. c-MWCNT improved the conductivity of PBT/PC blends and the percolation of c-MWCNT in the nanocomposites was 1.88 wt%. The dielectric constant was enhanced obviously when the c-MWCNT content was larger than P_c.

References

1. A. H. Tsou, C. R. López-Barrón, and P. Jiang, *Polymer,* **104**, 72 (2016).

2. J. H. Lee, K. Choi, and E. Kim, *Polym. Korea*, **35**, 543 (2011).

3. F. Wang, L. T. Drzal, Y. Qin, and Z. Huang, *Composites Part A,* **87**, 10 (2016).

4. D. Y. Wee, J. W. Han, and J. K. Choi, *Polym. Korea*, **37**, 420 (2013).

5. Z. Spitalsky, D. Tasis, K. Papagelis, and C. Galiotis, *Prog. Polym. Sci.,* **35**, 357 (2010).

6. G. Liu, *Polym. Korea*, **40**, 42 (2016).

7. C. P. Rejisha, S. Soundararajan, N. Sivapatham, and K. Palanivelu, *J. Polym.,* http://dx.doi.org/10.1155/2014/157137.

8. F. F. Wang, H. Wang, K. Zheng, L. Chen, X. Zhang, and X. Y. Tian, *Colloid Polym. Sci.,* **292**, 953 (2014).

9. L. M. Nanjegowda, R. Bommulu, V. Juikar, and S. Hatna, *Ind. Eng. Chem. Res.,* **52**, 5672 (2013).

10. R. M. Kooshki, I. Ghasemi, M. Karrabi, and H. Azizi, *J. Vinyl Addit. Technol.*, **19**, 203 (2013).

11. S. L. Sun, F. F. Zhang, Y. Fu, C. Zhou, and H. X. Zhang, *J. Macromol. Sci., Part B: Phys.*, **52**, 861 (2013).

12. R. Sonnier, A. Viretto, A. Taguet, and J. M. Lopez-Cuesta, *J. Appl. Polym. Sci.*, **125**, 3148 (2012).

13. P. R. Rajakumar and R. Nanthini, *Int. Let. Chem. Phys. Ast.,* **9**, 15 (2013).

14. K. Lee, J. Shin, H. Y. Yu, D. Kwak, C. K. Kim, and S. Ahn, *Polym. Korea*, **40**, 385 (2016).

15. T. T. Wen, Y. Guo, S. X. Song, S. L. Sun, and H. X. Zhang, *J. Polym. Res.*, **22**, 222 (2015).
16. Y. Guo, J. He, X. Zhang, S. Sun, and H. Zhang, *J. Macromol. Sci. Part B: Phys.*, **54**, 823 (2015).
17. Y. Guo, S. L. Sun, and H. X. Zhang, *Rsc. Adv.,* **4**, 58880 (2014).
18. B. Deng, Y. Guo, S. X. Song, S. L. Sun, and H. X. Zhang, *J. Polym. Res.*, **23**, 210 (2016).
19. M. K. Razieh, G. Ismail, and K. Mohammad, *Iran. J. Polym. Sci. Tech.*, **26**, 101 (2013).
20. W. S. Depolo and D. G. Baird, *Polym. Compos.,* **30**, 188 (2010).
21. M. Moniruzzaman and K. I. Winey, *Macromolecules*, **39**, 5194 (2006).
22. C. Y. Li, L. Li, W. Cai, S. L. Kodjie, and K. K. Tenneti, *Adv. Mater.*, **17**, 1198 (2005).
23. P. Yadav, A. K. Srivastava, M. K. Yadav, R. Kripal, V. Singh, and D. B. Lee, and J.-H. Lee, *Arab. J. Chem.*, in press, https://doi.org/10.1016/j.arabjc.2015.10.015.
24. S. Maiti, S. Suin, N. K. Shrivastava, and B. B. Khatua, *Synth. Met.*, **165**, 40 (2013).
25. O. Saligheh, M. Forouharshad, R. Arasteh, R. Eslami-Farsani, R. Khajavi, and B. Y. Roudbari, *J. Polym. Res.*, **20**, 65 (2013).
26. S. Maiti, S. Suin, N. K. Shrivastava, and B. B. Khatua, *J. Appl. Polym. Sci.*, **130**, 543 (2013).
27. Z. Y. Xiong, Y. Sun, L. Wang, Z. X. Guo, and J. Yu, *Sci. China.*

Chem., **55**, 808 (2012).
28. J. L. Li, X. F. Wang, C. J. Yang, J. H. Yang, Y. Wang, and J. H. Zhang, *Composites Part A*, **90**, 200 (2016).
29. B. Deng, H. Lv, S. Song, S. Sun, and H. Zhang, *J. Polym. Res.*, **24**, 85 (2015).
30. J. X. He, Y. Guo, S. L. Sun, and H. X. Zhang, *J. Polym. Eng.*, **35**, 247 (2015).
31. H. Bai, Y. Zhang, Y. Zhang, X. Zhang, and W. Zhou, *Polym. Test.*, **24**, 235 (2005).
32. M. E. Nichols and R. E. Robertson, *J. Polym. Sci., Part B: Polym. Phys.*, **30**, 755 (1992).
33. J. Kim, M. E. Ichols, and R. E. Robertson, *J. Polym. Sci., Part B: Polym. Phys.*, **32**, 887 (1994).
34. K. S. Nilesh, S. Supratim, M. Sandip, and B. K. Bhusan, *RSC Adv.*, **4**, 24584 (2014).
35. K. S. Nilesh, S. Supratim, M. Sandip, and B. K. Bhusan, *Ind. Eng. Chem. Res.*, **52**, 2858 (2013).
36. Y. Jiao, L. Yuan, G. Liang, and A. Gu, *J. Phys. Chem. C*, **118**, 24091 (2014).
37. J. X. Lu, K. S. Moon, J. W. Xu, and C. P. Wong, *J. Mater. Chem.*, **16**, 1543 (2006).
38. M. J. Jiang, Z. M. Dang, M. Bozlar, F. Miomandre, and J. B. Bai, *J. Appl. Phys.*, **106**, 084902 (2009).